

Coupled Lorenz systems, cusp maps, and the lowering of the second laser threshold

N. M. Lawandy, D. V. Plant, and Kayee Lee

Division of Engineering, Brown University, Providence, Rhode Island 02912

(Received 13 March 1986)

We have studied the behavior of two symmetrically coupled Lorenz systems in the parameter space where the uncoupled systems correspond to the bad-cavity limit of the single-mode laser model. The differential equations show that the threshold for the appearance of a strange attractor in the coupled system drops below the uncoupled value, exhibits a minimum at $\beta=0.5$, and then increases rapidly as $\beta \rightarrow 0.7$. We have also studied the use of coupled logistic cusp maps for predicting the initial drop in the second laser threshold. The results show good qualitative agreement for low β values ($\beta < 0.25$).

I. INTRODUCTION

The isomorphism of the mean-field model for a resonantly tuned single-model homogeneously broadened ring laser and the Lorenz equations were shown by Haken in 1975.¹ Unfortunately, the conditions for observing chaotic emission require the bad-cavity limit in conjunction with a large gain. Optically pumped far-infrared lasers, owing to their narrow linewidths and large gains, could serve as the experimental workhorse for the observation and study of optical chaos in the Lorenz system. These lasers, however, exhibit complicated intensity-dependent gain structure and therefore may introduce strong intensity-dependent sidebands and inhomogeneous broadening effects.² A key to the problem lies in the ability to drop the threshold for chaos in order that lower pump powers could result in the necessary gain for the transition to chaotic output.

With the above-stated motivation, we have considered the case of two coupled Lorenz systems. This is schematically shown in Fig. 1 where each ring system is in the mean-field limit.

II. COUPLED LORENZ SYSTEMS

The equations of motion for the unidirectionally coupled ring lasers (Lorenz systems) shown in Fig. 1 are given below:

$$\dot{X}_1 = \sigma Y_1 - \sigma(X_1 - \beta X_2), \quad (1a)$$

$$\dot{Y}_1 = RX_1 - Y_1 - X_1 Z_1, \quad (1b)$$

$$\dot{Z}_1 = X_1 Y_1 - b Z_1, \quad (1c)$$

$$\dot{X}_2 = \sigma Y_2 - \sigma(X_2 - \beta X_1), \quad (2a)$$

$$\dot{Y}_2 = RX_2 - Y_2 - X_2 Z_2, \quad (2b)$$

$$\dot{Z}_2 = X_2 Y_2 - b Z_2. \quad (2c)$$

These equations are coupled via a term common to lasers with injected fields.³ The coupling constant β controls the degree to which these systems interact and may be experimentally varied by reflection losses. The general problem

of coupled lasers does not require that there be a single coupling constant for one system's injection into the other. The case of equal coupling, however, is of interest as it preserves symmetry between the two systems.

The numerical integration of the coupled systems (1a)–(2c) was performed using a fifth-order Runge-Kutta algorithm on a Digital Equipment Corporation VAX11/730 computer. Noting that the equations share a common pump parameter R , the transition of one system into the second laser threshold R_{th} was determined as a function of the coupling constant β . The results of this analysis are shown in Fig. 2 for the case $\sigma=4$, $b=0.3$.

The threshold for chaos R_{th} was observed to drop from 10.5 at $\beta=0$ to a minimum of 6.5 for $\beta=0.5$. Increasing the coupling beyond this point resulted in a rapid rise of the excitation required to reach the chaos threshold. The rapid increase of R_{th} in the region $0.5 \leq \beta \leq 0.7$ is accurately given by

$$R_{th} = e^{n(\beta)}, \quad (3)$$

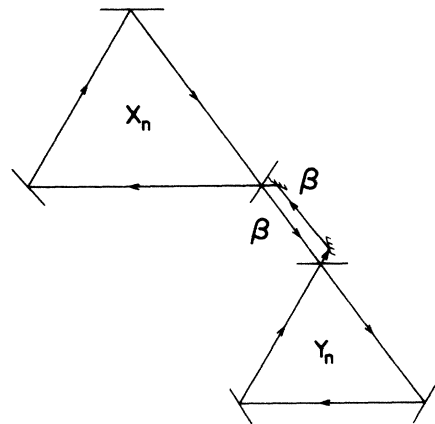


FIG. 1. Two coupled Lorenz lasers.

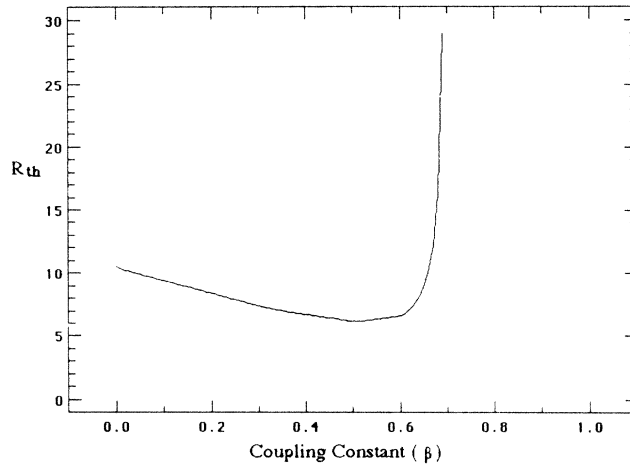


FIG. 2. Threshold excitation for the onset of chaos as a function of coupling constant [numerical integration of Eqs. (1a)–(2c)].

where $n(\beta) = a_0 + a_1\beta + a_2\beta^2 + a_3\beta^3 + a_4\beta^4$,

$$a_0 = 11092.1,$$

$$a_1 = -70378.2,$$

$$a_2 = 167465.0,$$

$$a_3 = -177100.0,$$

$$a_4 = 70238.9.$$

III. COUPLED LOGISTIC MAPS

The use of logistic maps for studying the dynamics of nonlinear systems has become very popular since the discoveries of Feigenbaum.⁴ The quadratic map bifurcation sequence has been verified in physical systems, such as the driven varactor diode *LRC* circuit.^{5–7} The use of logistic maps in quantum optics has been primarily motivated by the work of Ikeda.⁸ Apart from this suggestion, based only on phase-reproducibility arguments, there has been very little work on the subject.

The Lorenz equations [(1a)–(1c) with $\beta=0$] have been

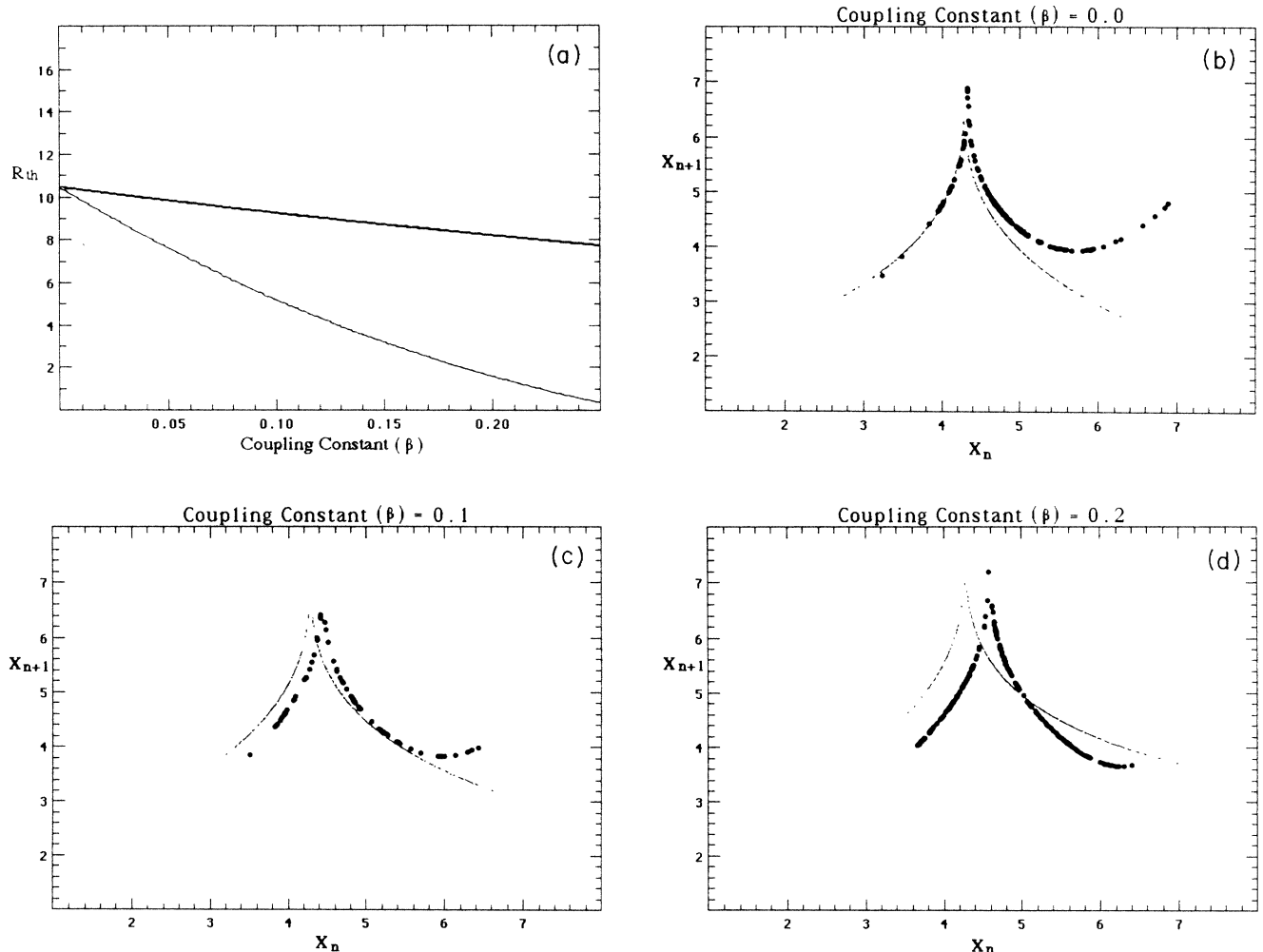


FIG. 3. (a) R_{th} vs β for the coupled logistic maps and the numerically integrated Eqs. (1a)–(2c); (b)–(d) comparison of the return map for the coupled cusps (small points) and the maximal values X_n obtained from the numerically integrated coupled equations with coupling constant (b) $\beta=0.0$, (c) $\beta=0.1$, and (d) $\beta=0.2$, respectively. The cusp parameters are those of Eq. (6) in the text.

studied numerically and have shown that in certain parameter spaces, the maximal values of the electric field X_n for trajectories near the nonwandering set result in Logistic maps having the form of a cusp.⁹⁻¹¹

The numerical solutions for the successive maximal values X_n of the uncoupled Lorenz equations result in X_{n+1} versus X_n curves shown in Fig. 3(b) (large dots). These cusps have been fitted by the logistic map:

$$X_{n+1} = \gamma(R)[X_n - a(R)]^{0.33} + b(R), \quad (4)$$

for the region $1 < R \leq 24$. The cusp fitting parameters γ , a , and b are all functions of the excitation parameter R .

Studies of coupled quadratic logistic maps have been previously performed.¹²⁻¹⁴ The work in Refs. 12 and 13 has been concerned with the parabolic map, the onset of crises, hysteresis, and irregular behavior due to coupling. The connection between the coupled maps and physical systems had not been made prior to the experimental study of coupled nonlinear oscillator circuits by Lawandy *et al.*¹⁴ In this work it was conjectured that the lowered chaos threshold predicted by the coupled parabolic maps might be observed in coupled varactor diode circuits. This effects was qualitatively observed as well as a stabi-

lizing effect which caused the coupled systems to remain locked and stable.

We have compared the numerical integration of the six coupled equations 1(a)–2(c) to the results of coupled cusp maps. This was motivated by the discovery that the maximal values $X_n^{1,2}$ of the coupled system also resulted in cusp logistic maps.

The approach to the problem of coupled logistic maps involved the study of the following equations:

$$\begin{aligned} X_{n+1} &= \gamma(R)[X_n - a(R)]^{0.33} + b(R) + \beta Y_n, \\ Y_{n+1} &= \gamma(R)[Y_n - a(R)]^{0.33} + b(R) + \beta X_n, \end{aligned} \quad (5)$$

where $0 \leq \beta \leq 1.0$. The coupled logistic maps displayed a lowering of the critical pump parameter R_{th} for the onset of chaos only over the region $0 < \beta < 0.25$. The cusp fitting parameters were found to be well approximated by linear functions of R . A variation of the cusp parameters resulted in a variation of both the slope and the $\beta=0$ intercept of the $R_{th}(\beta)$ for the coupled logistic maps. The equations for the cusp parameters which gave an $R_{th}=10.5$ are given by

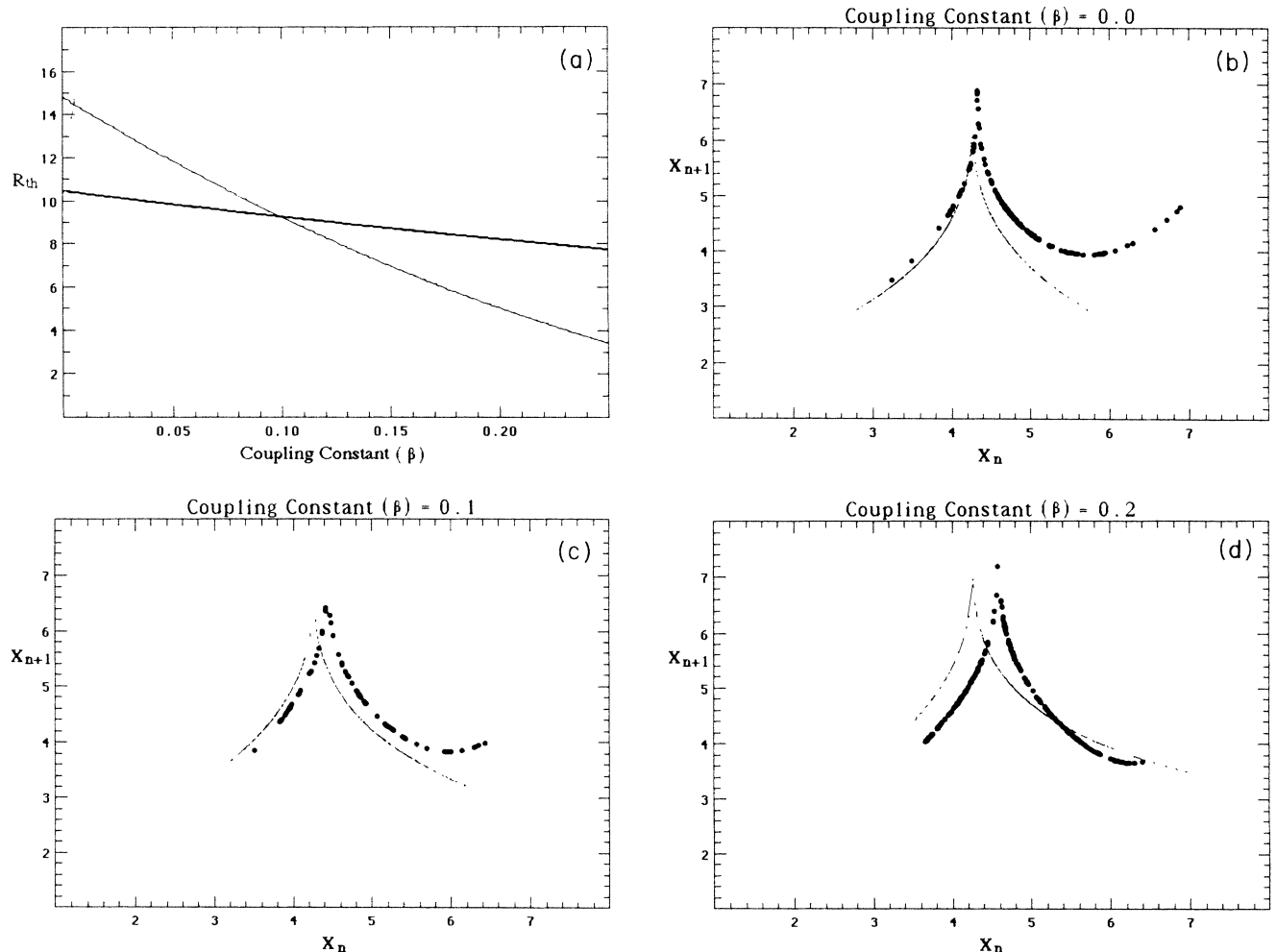


FIG. 4. (a) Comparison of R_{th} vs β for the coupled logistic maps and the numerically integrated equations (1a)–(2c) for a different set of cusp fitting parameters; (b)–(d) comparison of the return map for the coupled cusps (small points) and the maximal values X_n obtained from the numerically integrated coupled equations with (b) $\beta=0.0$, (c) $\beta=0.1$, and (d) $\beta=0.2$, respectively.

$$\begin{aligned}
 \gamma(R) &= 1.725 + 0.875R, \\
 a(R) &= 2.7508 + 0.08497R, \\
 b(R) &= 3.0327 + 0.2157R.
 \end{aligned}
 \tag{6}$$

Figure 3(a) shows the R_{th} -versus- β curve for the coupled logistic maps which resulted in $R_{th} = 10.5$ for $\beta = 0$ (uncoupled case). Figures 3(b)–3(d) show a comparison of the X_{n+1} -versus- X_n plots which result from the coupled cusps and the successive maximal values X_n obtained by numerical integration of the system of equations 1(a)–2(c). The figure set 4(a)–4(d) shows the same comparisons but the different $\gamma(R)$, $a(R)$, and $b(R)$ parameters. It is clear that, in the weak-coupling limit, the coupled logistic maps produce good qualitative agreement with the numerical integration of the six coupled Lorenz equations.

IV. CONCLUSIONS

We have shown that coupling two Lorenz systems ($b = 0.3, \sigma = 4$) results in an initial lowering of the second laser threshold with an increase in the coupling constant up to $\beta = 0.5$. Beyond this point, the second threshold increases rapidly and diverges as $\beta \rightarrow 0.70$. This effect

shows that coupled chaotic systems may display either increased sensitivity to perturbations or a greatly enhanced stability as a function of coupling.

In addition, we have studied the use of coupled logistic maps to approximate the behavior of two coupled Lorenz systems. We have found that the maximal values of the electric field X_n of the coupled differential equations also display a cusp return map structure. Coupled curve fitted cusps which approximate the uncoupled system, were found to approximate the cusps obtained from the numerical solution of the coupled Lorenz systems. The coupled logistic cusp maps displayed a lowering of the instability threshold for small coupling constants ($\beta \leq 0.25$). The agreement between the coupled logistic maps and the coupled differential equations may be improved by higher-order fits of the cusp parameters as a function of R . We are currently exploring the coupling of two Lorenz systems operating the self-pulsing regime ($\beta < 0.21, \sigma \leq 4$), as well as systems with unequal coupling.

ACKNOWLEDGMENTS

This work was supported by the Alfred P. Sloan Foundation and the National Science Foundation under Grant No. ENG-8451099.

¹H. Haken, *Phys. Lett.* **53A**, 77 (1975).

²N. M. Lawandy, *J. Opt. Soc. Am. B* **2**, 108 (1985).

³D. K. Bandy, L. M. Narducci, L. A. Lugiato, *J. Opt. Soc. Am. B* **2**, 148 (1985).

⁴M. J. Feigenbaum, *J. Stat. Phys.* **19**, 25 (1978).

⁵P. S. Linsay, *Phys. Rev. Lett.* **47**, 1349 (1981).

⁶J. Testa, J. Perez, and C. Jeffries, *Phys. Rev. Lett.* **48**, 714 (1982).

⁷R. W. Rollins and E. R. Hunt, *Phys. Rev. Lett.* **49**, 1295 (1982).

⁸K. Ikeda, *Opt. Commun.* **30**, 257 (1979).

⁹E. N. Lorenz, *J. Atmos. Sci.* **20**, 130 (1963).

¹⁰E. N. Lorenz, *Global Analysis*, Vol. 755 of *Lecture Notes in Mathematics*, edited by M. Grmelo and J. Marsden (Springer-Verlag, Berlin, 1979).

¹¹E. N. Lorenz, *Ann. N.Y. Acad. Sci.* **357**, 282 (1980).

¹²Y. Gu, M. Tung, J. M. Yuan, D. M. Feng, and L. M. Narducci, *Phys. Rev. Lett.* **52**, 701 (1984).

¹³J. M. Yuan, M. Tung, D. H. Feng, and L. M. Narducci, *Phys. Rev. A* **28**, 1662 (1983).

¹⁴N. M. Lawandy and D. V. Plant, *Digest of the Conference on Instabilities and Dynamics of Lasers and Nonlinear Optical Systems*, Rochester 1985 (unpublished).